ARTICLE IN PRESS

Cytotherapy 000 (2023) 1–15



Contents lists available at ScienceDirect

CYTOTHERAPY



journal homepage: www.isct-cytotherapy.org

Full-length article

Bone mesenchymal stromal cell-derived small extracellular vesicles inhibit inflammation and ameliorate sepsis via delivery of microRNA-21a-5p

Ruichao Niu^{1,2,3,4,5,6,7,*}, Pinhua Pan^{1,2,3,4,5,6,*}, Chonghui Li⁸, Baihua Luo⁹, Hua Ma¹⁰, Haojie Hao¹¹, Zhigang Zhao¹², Hang Yang^{1,2,3,4,5,6}, Shiyang Ma^{1,2,3,4,5,6}, Fei Zhu^{1,2,3,4,5,6}, Jie Chen^{1,2,3,4,5,6,**}

ARTICLE INFO

Article History: Received 14 October 2022 Accepted 4 February 2023 Available online xxx

Key Words: inflammation mesenchymal stromal cells microRNA-21a-5p sepsis small extracellular vesicles

ABSTRACT

Background aims: Sepsis is a potentially life-threatening disease that results from a severe systemic inflammatory response due to infection. Mesenchymal stromal cell-derived small extracellular vesicles (MSC sEVs) are able to transfer bioactive molecules and have been demonstrated to play an important role in the pathophysiological process of sepsis. Herein the authors aimed to investigate the potential role and downstream molecular mechanism of MSC sEVs in sepsis.

Methods: MSC sEVs were acquired by ultracentrifugation and then injected into a cecal ligation and puncture mouse model. The efficacy of MSC sEVs in both *in vitro* and *in vivo* models of sepsis was evaluated.

Results: MSC sEV therapy improved survival, reduced sepsis-induced inflammation, attenuated pulmonary capillary permeability and improved liver and kidney function in septic mice. In addition, the authors found that microRNA-21a-5p (miR-21a-5p) was highly enriched in MSC sEVs, could be transferred to recipient cells, inhibited inflammation and increased survival in septic mice. Furthermore, the authors demonstrated that MSC sEV miR-21a-5p suppressed inflammation by targeting toll-like receptor 4 and programmed cell death 4. The therapeutic efficacy of MSC sEVs was partially abrogated by transfection with miR-21a-5p inhibitors. Conclusions: Collectively, the authors' data suggest that miR-21a-5p-bearing MSC sEVs may be a prospective and effective sepsis therapeutic strategy.

© 2023 International Society for Cell & Gene Therapy. Published by Elsevier Inc. This is an open access article under the CC BY-NC-ND license (http://creativecommons.org/licenses/by-nc-nd/4.0/)

Introduction

Sepsis is a potentially life-threatening disease that results from a severe systemic inflammatory response to infection [1]. The pathogenesis of sepsis involves excessive activation of inflammatory cells such as macrophages, uncontrolled systemic inflammation and dysfunction of multiple organs [2]. Although continuous progress has been made regarding the therapeutic principles, sepsis remains the

¹ Department of Respiratory Medicine, National Key Clinical Specialty, Branch of National Clinical Research Center for Respiratory Disease, Xiangya Hospital, Central South University, Changsha, China

² Center of Respiratory Medicine, Xiangya Hospital, Central South University, Changsha, China

³ Clinical Research Center for Respiratory Diseases in Hunan Province, Changsha, China

⁴ Hunan Engineering Research Center for Intelligent Diagnosis and Treatment of Respiratory Disease, Changsha, China

⁵ National Clinical Research Center for Geriatric Disorders, Xiangya Hospital, Central South University, Changsha, China

⁶ Department of Respiratory Medicine, Second Affiliated Hospital of Xinjiang Medical University, Urumqi, China

Department of Hepatobiliary Surgery, Chinese People's Liberation Army General Hospital, Chinese People's Liberation Army Medical College, Beijing, China

⁸ Institute of Hepatobiliary Surgery, Chinese People's Liberation Army General Hospital, Chinese People's Liberation Army Medical College, Beijing, China

⁹ Department of Pathology, Xiangya Hospital, Central South University, Changsha, China

¹⁰ Department of Infectious Disease, People's Hospital of Liuyang City, Liuyang, China

¹¹ Institute of Basic Medicine Science, Chinese People's Liberation Army General Hospital, Chinese People's Liberation Army Medical College, Beijing, China

¹² Center of Pulmonary and Critical Care Medicine, Chinese People's Liberation Army General Hospital, Chinese People's Liberation Army Medical College, Beijing, China

^{**} Correspondence: Jie Chen, PhD, Department of Respiratory Medicine, National Key Clinical Specialty, Branch of National Clinical Research Center for Respiratory Disease, Xiangya Hospital, Central South University, No. 28 Xiangya Road, Kai-Fu District, Changsha 410008, China.

E-mail address: chenjie869@163.com (J. Chen).

^{*} These authors contributed equally to this work.

leading cause of death among patients admitted to intensive care units [3]. Currently, the mortality rate of sepsis is approximately 26% [3,4]. Therefore, novel therapeutics for sepsis that target specific pathologies to prevent disease progression are urgently needed.

To date, several pre-clinical studies have recognized mesenchymal stromal cells (MSCs) as a novel tool for sepsis therapy via their ability to inhibit the overwhelming inflammatory response [5–7]. Moreover, MSCs have been demonstrated in two clinical trials to offer therapeutic benefits for sepsis [8,9]. The underlying mechanisms of the beneficial effects of MSCs on sepsis remain under exhaustive investigation. Interestingly, growing pre-clinical data have indicated that MSCs exert their restorative effects through paracrine mechanisms instead of cell engraftment [10,11]. This so-called paracrine hypothesis has attracted considerable interest in the scientific community. Currently, the authors and others have demonstrated that MSC-conditioned medium can inhibit excess pro-inflammatory responses and repair sepsis-induced lung injury both *in vitro* and *in vivo* [12,13].

Recently, MSCs have been demonstrated to release paracrine mediators such as extracellular vesicles (EVs), which play an active role in a variety of diseases [14-17]. EVs are natural nano- to microsized membrane vesicles encapsulated by phospholipid bilayers that are released by all cell types into the extracellular environment [18]. According to the Minimal Information for Studies of Extracellular Vesicles guidelines, EVs are generally categorized into two major subclasses: medium to large EVs (range, 150-1000 nm) and small EVs (sEVs) (approximately 30–150 nm) [19]. EVs have emerged as important mediators of intercellular communication for physiological and pathological processes as a result of their collection of biologically active factors, including proteins, messenger RNAs (mRNAs) and microRNAs (miRNAs) [18]. MSC-derived EVs have significant potential for cell-free cell therapy in the field of regenerative medicine. They can avoid the side effects of the entire MSC injection process, including quality assurance challenges, senescence-induced genetic instability, tumor generation and immune rejection [20]. Regarding the field of sepsis, numerous studies have reported the therapeutic effects of MSC-derived EVs in several types of sepsis-induced organ dysfunction, such as acute lung injury [21–23], acute kidney injury [24], cardiovascular disorder [25,26] and liver injury [27]. However, the underlying mechanisms involved remain only partially understood.

In this study, the authors explored the effect of MSC sEVs on survival, organ failure and inflammation in a cecal ligation and puncture (CLP) septic mouse model. Moreover, the authors evaluated the impact of MSC sEVs on the inflammatory response of macrophages *in vitro*. The authors observed that miRNA-21a-5p (miR-21a-5p) was enriched in MSC sEVs. The authors then explored the role of MSC sEV-derived miR-21a-5p in the inflammatory response of macrophages and in CLP mice. The authors' data confirmed the important role of MSC sEV-derived miR-21a-5p in sepsis and suggested that it may provide insights into novel therapies for sepsis.

Methods

Animals

All animal experiments were performed according to National Institutes of Health (NIH) guidelines (NIH publication no. 85–23, revised 1996) and laboratory animal management regulations in China and adhered to the 2011 Guide for the Care and Use of Laboratory Animals published by the NIH. The protocol was approved by the ethics committee of Xiangya Hospital of Central South University (201603218).

Extraction and identification of MSC sEVs

Bone MSCs were isolated from mice as described in the authors' previous study [28]. A differential ultracentrifugation method was applied to extract MSC sEVs based on the method of Théry *et al.* [29]. Details of the operational process for sEV extraction are schematically shown in Figure 1A. Briefly, when MSCs at passage three grew to 70% fusion, they were cultured with serum-free medium (Cyagen

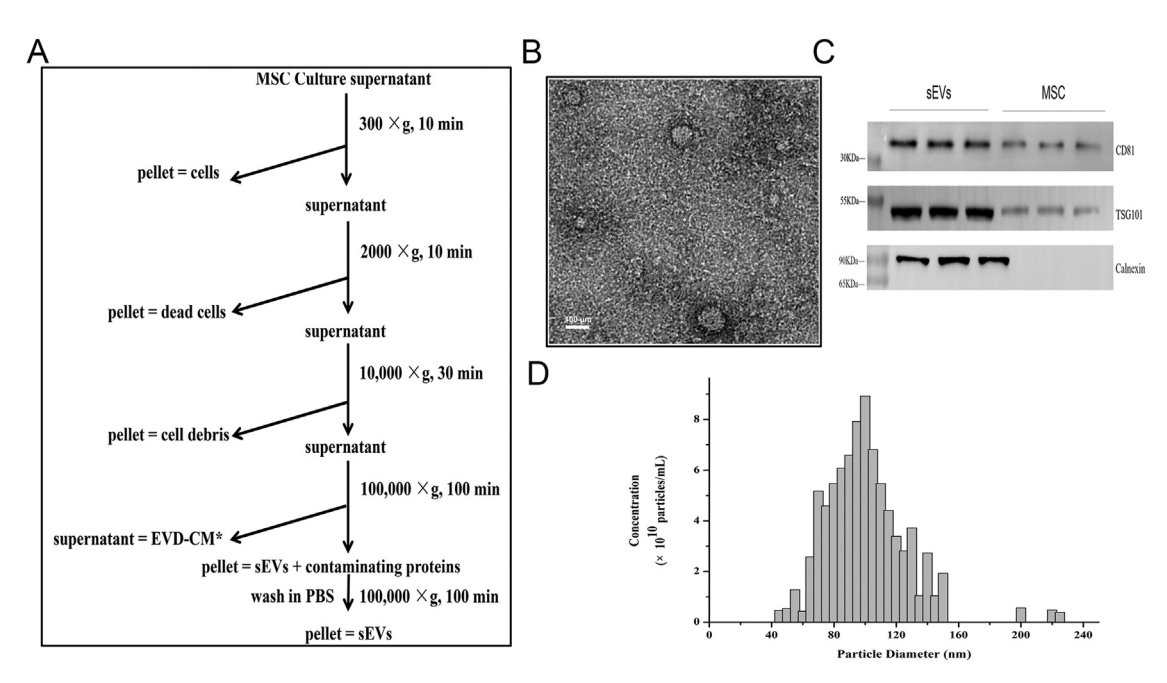


Fig. 1. Isolation and characterization of MSC sEVs. (A) Schematic representation of MSC sEV isolation using differential ultracentrifugation based on the method of Théry *et al.* [29]. The speed and length of each centrifugation are indicated to the right of the arrows. All centrifugation steps were performed at 4°C. (B) Transmission electron micrographs of purified MSC sEVs showing a spheroid shape (scale bar = 100 nm). (C) Western blotting results indicating the positive expression of CD81 and TSG101 proteins and negative expression of calnexin in sEVs derived from MSCs. (D) The number of particles versus particle size was generated using nanoparticle tracking analysis with a ZetaView. Results are presented as the mean of three independent experiments.

Biosciences Inc, Guangzhou, China). Every other day, the supernatant of the cultured MSCs was collected and centrifuged for at least 10 min at 300 \times g and further centrifuged for 10 min at 2000 \times g. The supernatant was then centrifuged for 30 min at $10\,000 \times g$ and filtered through $0.22-\mu m$ filters to remove cell debris. Finally, the supernatant was ultracentrifuged at 100 000 × g for 100 min. To purify the sEVs, the pellets were washed with phosphate-buffered saline (PBS) and centrifuged again at $100\,000 \times g$ for 100 min. After this step, the pellets were diluted with PBS and kept at -80° C for subsequent experiments. All of the aforementioned procedures were performed at 4°C. Protein concentrations of the sEVs were evaluated using a bicinchoninic acid protein assay kit (Thermo Fisher Scientific, Waltham, MA, USA). Additionally, the sEV ultrastructure was analyzed by transmission electron microscopy (H-7650; Hitachi, Tokyo, Japan). The size distribution and concentration of the particles were analyzed with a nanoparticle tracking analyzer (ZetaView; Particle Metrix GmbH, Inning am Ammersee, Germany). Protein markers such as CD81 (primary antibody, 1:300, ab79559; Abcam, Cambridge, UK), TSG101 (primary antibody, 1:1000, ab125011; Abcam) and calnexin (primary antibody, 1:200, sc23954; Santa Cruz Biotechnology, Inc, Santa Cruz, CA, USA) were assessed by western blot.

Induction and treatment of sepsis

Male C57BL/6 mice aged 7–8 weeks were kept in specific pathogen-free conditions with stable room temperatures (23 \pm 2°C). CLP was performed as previously described [5]. In brief, mice were anesthetized using an intraperitoneal injection of pentobarbital (90 mg/kg). The cecum was ligated at the colon juncture with a 4-0 silk ligature suture and then penetrated twice using a 21-gauge needle. Immediately after surgery, all mice were resuscitated with a subcutaneous injection of pre-warmed normal saline (35 mL/kg). In the sham operation group, the cecum was exteriorized but not ligated or punctured. Mice that underwent sham or CLP surgery were injected through the tail vein with either saline (150 μ L) or MSC sEVs (40 μ g per mouse in 150 μ L of saline). Then, some of the mice were killed 48 h after the sham or CLP procedure for subsequent analysis. The other mice were monitored every 12 h for seven days for survival rate analysis, (Figure 2A).

Histopathological analysis

All liver, lung and kidney tissues were harvested and then fixed in 4% paraformaldehyde. After gradual dehydration, all samples were embedded in paraffin and cut into 4- to 6- μ m-thick sections for hematoxylin and eosin staining. All tissue sections were observed under an Eclipse E800 microscope (Nikon, Tokyo, Japan). Six slides per tissue were examined. At least 10 visual fields were randomly selected. Tissue injury scores were evaluated by two investigators in a blinded manner according to the published scoring system [30].

Bacterial clearance assessment, organ function measurement and cytokine/chemokine determination

Mouse plasma was collected 48 h after the CLP or sham operation. Measurement of bacterial clearance was performed on peritoneal lavage fluid and plasma. After 10-fold dilution, samples were plated on blood agar plates for 24 h at 37°C. The number of colony-forming units (CFUs) per milliliter of peritoneal lavage fluid or plasma was then counted.

Plasma levels of alanine aminotransferase (ALT), aspartate aminotransferase (AST) and bilirubin were used to assess liver dysfunction, and blood urea nitrogen (BUN) and creatinine were used to assess kidney dysfunction. Amylase was used as an indicator of pancreatic dysfunction. Commercially available kits (BioAssay Systems, Atlanta, GA, USA) and a Photometer 5010 (ROBERT RIELE GmbH & Co KG,

Berlin, Germany) were used to measure plasma levels of ALT, AST, bilirubin, amylase, BUN and creatinine based on the manufacturers' instructions. Plasma levels of tumor necrosis factor alpha (TNF- α), IL-1 β , IL-6 and IL-10 were assessed by mouse cytokine and chemokine enzyme-linked immunosorbent assays (R&D Systems Inc, Minneapolis, MN, USA) based on the manufacturer's instructions.

Assessment of lung wet:dry weight ratio and analysis of bronchoalveolar lavage fluid

To measure the total amount of lung water, the left lung of the mice was excised and weighed to measure the wet weight. Next, the left lung tissues were placed in an oven at 60°C. After 48 h, the tissues were reweighed to measure the dry weight. The lung wet:dry ratio was measured as described in the authors' previous study [28].

Bronchoalveolar lavage was performed according to a previously published protocol [28]. Bronchoalveolar lavage fluid (BALF) samples were centrifuged at 500 \times g for 10 min at 4°C. A bicinchoninic acid protein assay kit was used to evaluate protein in the BALF. The cell pellet in BALF was resuspended in 100 μ L of PBS. After Wright—Giemsa staining (Beijing Solarbio Science & Technology Co, Ltd, Beijing, China), neutrophil cells were counted under a microscope.

Bone marrow-derived macrophage isolation and treatment

Bone marrow-derived macrophages (BMDMs) were isolated from the bone marrow of male C57BL/6 mice aged 6–8 weeks. In brief, mouse bone marrow was extracted, rinsed with PBS and passed through a 200 mesh sieve. After removing the red blood cells, the precipitate was cultured in complete Roswell Park Memorial Institute 1640 medium with 25 ng/mL macrophage colony-stimulating factor for 5 days in a 37°C and 5% carbon dioxide incubator. Lipopolysaccharide (LPS) 100 ng/mL (Sigma-Aldrich, St Louis, MO, USA) was used to stimulate the BMDMs for 24 h. Different doses of MSC sEVs (1 μ g, 2 μ g and 4 μ g per 1 × 10⁵ cells in 10 μ L of PBS) were applied to the BMDM culture medium. The authors found that there was a dose effect on miR-21a-5p expression with increasing amounts of sEVs *in vitro*. A total of 20 μ g of MSC sEVs provided protective effects (see supplementary Figure 1). Therefore, the authors chose this dose for subsequent experiments *in vitro*.

MSC sEV labeling and uptake

To determine whether BMDMs could take up MSC sEVs, the authors labeled MSC sEVs with 1,1'-dioctadecyl-3,3,3',3'-tetramethy-lindocarbocyanine perchlorate (Dil) (D282; Thermo Fisher Scientific). Subsequently, LPS-treated BMDMs were co-cultured with Dil-labeled sEVs at 37°C for 24 h. Thereafter, BMDMs were rinsed with PBS and fixed in 4% paraformaldehyde. After permeabilization with ice-cold methanol for 15 min, BMDMs were stained on glass slides with Alexa Fluor 647 phalloidin (A22287) and 4',6-diamidino-2-phenylindole (D1306) (Thermo Fisher Scientific). The cells were then observed under a confocal laser scanning microscope (LSM 800; Carl Zeiss Microscopy GmbH, Jena, Germany).

To trace the administered MSC sEVs *in vivo*, the authors injected Dil-labeled sEVs into mice through the tail vein. For immunofluorescence staining, fixed frozen sections of mouse lung were incubated with rat anti-mouse F4/80 monoclonal antibody (ab6640; Abcam) at $10~\mu g/mL$ overnight at 4°C. After washing the slides in PBS, the slides were incubated with anti-rat lgG secondary antibody (ab150157; Abcam) and 4′,6-diamidino-2-phenylindole at room temperature. Next, images were acquired with a confocal laser scanning microscope (LSM 800). To quantify the retention of MSC sEVs, the number of nuclei of F4/80-positive cells surrounded by Dil-labeled MSC sEVs

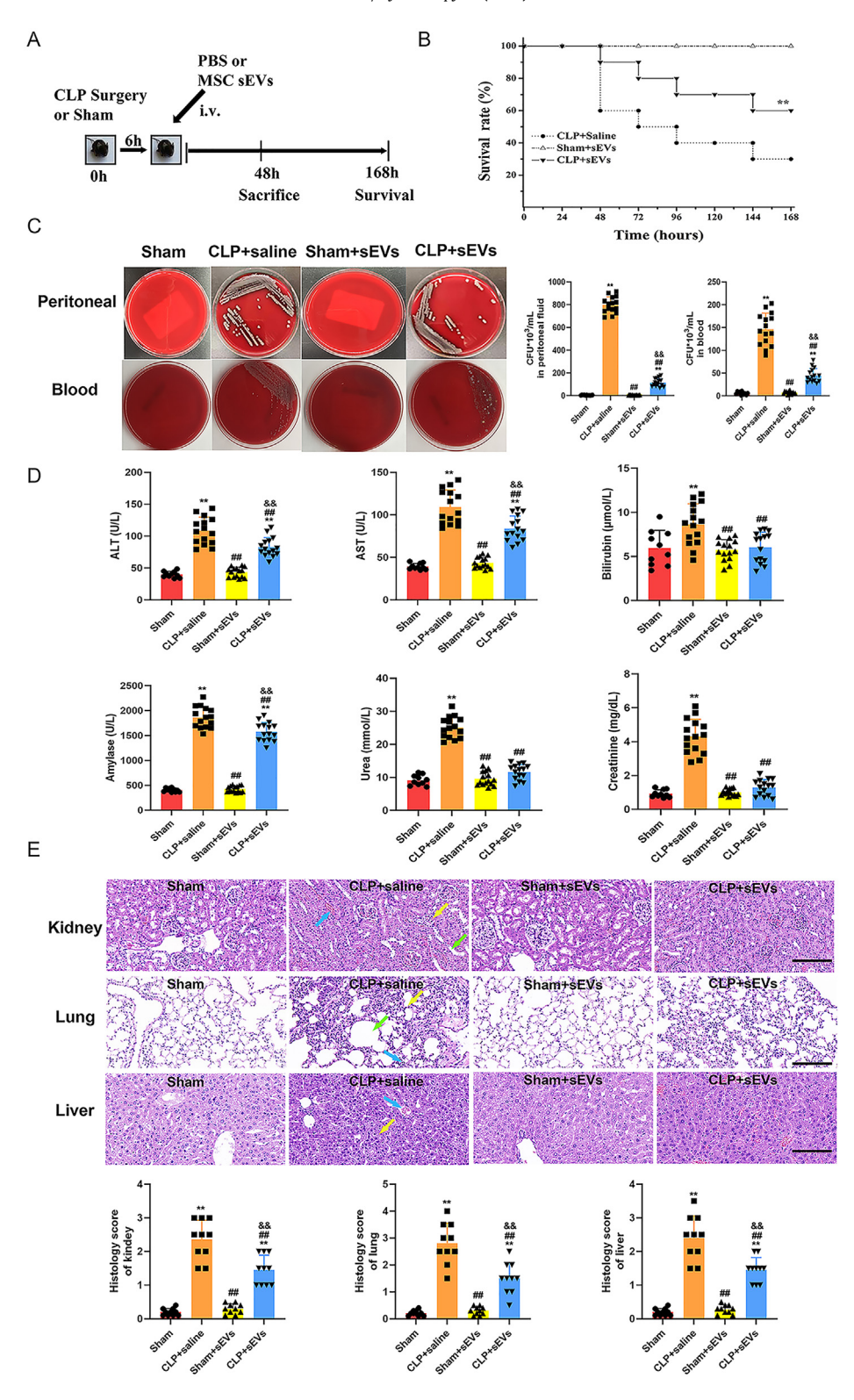


Fig. 2. MSC sEVs improved survival and attenuated organ injury in septic mice. (A) Experimental design for the *in vivo* study. Sham-operated mice underwent the same procedure without ligation and puncture of the cecum. Saline or MSC sEVs (40 μ g per mouse in 150 μ L of saline) were injected through the tail vein 6 h after the CLP operation. Mice were then killed 48 h later to evaluate therapeutic efficacy or observed for 168 h (7 days) to evaluate survival rate. (B) Kaplan—Meier survival curves showing that administration of MSC sEVs significantly improved survival in mice with CLP-induced sepsis at 168 h (n = 15–20 mice per group, **P < .01, compared between the CLP+sEVs and CLP+Saline groups). (C) Bacterial counts in peritoneal fluid and peripheral blood (n = 15 for each group). (D) Organ dysfunction biomarkers AST, ALT, bilirubin, amylase, BUN and creatinine measured in plasma (n = 15 for each group). (E) Sections were stained with hematoxylin and eosin and examined histologically. The representative sections are shown at ×200 original magnification (scale bar = 50 μ m). With regard to kidney histology, the yellow arrow indicates a shrunken glomerulus; the green arrow indicates tubular injury, including brush border loss and tubular luminal debris or obstruction; and the blue arrow indicates capillary congestion. Regarding lung histology, the yellow arrow indicates alveolar wall thickening, the blue arrow indicates infiltrated inflammatory cells in the alveoli and the green arrow indicates an enlarged interstitial space. With respect to liver histology, the yellow arrow indicates hepatic cell edema and the blue arrow indicates capillary congestion. Histological injury scores are shown at the bottom (n = 15 for each group). Statistical analysis was performed using one-way ANOVA with a Tukey—Kramer post-hoc test. Results are presented as mean ± SD. ANOVA, analysis of variance; SD, standard deviation. ANOVA, analysis of variance; SD, standard deviation.

was divided by the total amount of nuclei of F4/80-positive cells. Five random tissue sections were selected per mouse.

miR-21a-5p mimics and inhibitor transfection

miR-21a-5p mimics (50 nM) or inhibitors (50 nM) and their negative controls (50 nM) (Guangzhou RiboBio Co, Ltd, Guangzhou, China) were transfected into MSCs using HiPerFect transfection reagent (QIAGEN, Germantown, MD, USA) following the manufacturer's instructions. After 6 h of transfection, the culture medium was changed to serum-free medium. After 42 h, sEVs were extracted according to the protocol shown in Figure 1A. The collected sEVs were used for subsequent experiments. miR-21a-5p mimics (50 nM) or inhibitors (50 nM) and their negative controls (50 nM) were also transfected into BMDMs using HiPerFect transfection reagent. The treatment grouping was as follows: mimic negative control (mimic NC), miR-21a-5p mimic (miR-21a-5p mimic), inhibitor negative control (inhibitor NC) and miR-21a-5p inhibitor (miR-21a-5p inhibitor).

Toll-like receptor 4, programmed cell death 4 and clathrin heavy chain inhibitor transfection

To determine whether inhibiting the expression of toll-like receptor 4 (TLR4) and programmed cell death 4 (PDCD4) in BMDMs had an effect on inflammation similar to that of MSC sEVs, the authors used small interfering RNAs (siRNAs). To determine whether inhibiting the expression of toll-like receptor 4 (TLR4) and programmed cell death 4 (PDCD4) in BMDMs had an effect on inflammation similar to that of MSC sEVs, the authors used small interfering RNAs (siRNAs). To find the highest inhibitory efficiency of siRNA, the authors purchased three TLR4 siRNAs (siTLR4 #1, #2 and #3) and three PDCD4 siRNAs (siPDCD4 #1, #2 and #3) from Guangzhou RiboBio Co, Ltd. Clathrin heavy chain was demonstrated to play an important role in endocytosis by macrophages [31]. Therefore, to confirm that increased miR-21a-5p in BMDMs was due to internalization of sEVs, siClathrin (see supplementary Table 2) was used to block the uptake of sEVs. BMDMs were transfected with siTLR4, siPDCD4, siClathrin or universal negative control siRNA using Lipofectamine 2000 (Thermo Fisher Scientific) based on the recommended protocol. After 24 h of transfection, the inhibitory efficiency was measured by quantitative realtime polymerase chain reaction (qRT-PCR). siRNAs with the highest inhibitory efficiency were selected for subsequent experiments. To validate the effect of siTLR4, the authors used a pharmacological inhibitor of TLR4 (TAK-242). BMDMs were treated with 100 ng/mL LPS with and without 1-h pre-treatment with 1 μ M TAK-242.

TLR4 and PDCD4 overexpression transfection

Lentiviral particles of TLR4 and PDCD4 overexpression and their negative controls were purchased from Shanghai GenePharma Co, Ltd (Shanghai, China). BMDMs were infected with a multiplicity of infection of 50 according to the manufacturer's protocol. BMDMs were divided into the following treatment groups: PBS (control), LPS + oe-NC (overexpressed TLR4 or PDCD4 control) + sEVs (mimic-NC), LPS + oe-NC (overexpressed TLR4 or PDCD4 control) + sEVs (miR-21a-5p mimic), LPS + oe-TLR4 or PDCD4 + sEVs (mimic-NC) and LPS + oe-TLR4 or PDCD4 + sEVs (miR-21a-5p mimic).

Plasmid construction and luciferase reporter assay

miR-21-5p binding sites in the TLR4 3' and PDCD4 3' untranslated region (UTR) sequences were cloned into a pGL3 luciferase control reporter vector (Promega Corporation, Madison, WI, USA). The desired pGL3-TLR4-wt or pGL3-TLR4-mut, pGL3-PDCD4-wt or pGL3-PDCD4-mut and miR-21-5p mimic or mimic-NC were delivered together into HEK293T cells (Shanghai Institute of Nutrition and

Health, Chinese Academy of Sciences, Shanghai, China). After 24 h of transfection, the cells were collected and measured for luciferase activity with the Dual-Luciferase Reporter Assay System (Promega Corporation).

RNA pull-down

The biotin-labeled miR-21a-5p mimic, biotin-labeled mutated miR-21a-5p and negative control were transfected into BMDMs. After 48 h, the cells were harvested and lysed, and the lysate was incubated with M-280 streptavidin magnetic beads (Thermo Fisher Scientific) at room temperature for 15—30 min. Next, qRT-PCR was carried out to analyze enrichment of the co-deposited TLR4 and PDCD4 RNA.

Ouantitative real-time PCR

Total RNA was purified from cultured cells or lung tissues using TRIzol reagent (Thermo Fisher Scientific) [28]. The primers used are displayed in Table 1. sEV miRNAs were extracted with the SeraMir Exosome RNA Purification Kit (System Biosciences, LLC, Palo Alto, CA, USA). The miRNA primers were supplied by Tiangen Biotechnology Co, Ltd (Beijing, China). RNA was converted to complementary DNA using a reverse transcription kit (QIAGEN). Next, qRT-PCR analysis was performed with SYBR Green Master Mix (Thermo Fisher Scientific) and run on a StepOne Plus Real-Time PCR System (Thermo Fisher Scientific). Data were analyzed with the $2^{-\Delta\Delta Ct}$ comparative method using U6 small nuclear RNA or glyceraldehyde 3-phosphate dehydrogenase for normalization.

Western blotting analysis

Total protein was purified from cells and lung tissue homogenate [32]. The protein was loaded on a 10% denaturing sodium dodecyl sulfate—polyacrylamide gel and then transferred to polyvinylidene fluoride membranes. After incubation with antibodies such as TLR4 (ab13867, 1:1000; Abcam), PDCD4 (ab51495, 1:1000; Abcam), phosphorylated nuclear factor kappa B (NF- κ B) p65 (#3033, 1:1000; Cell Signaling Technology, Danvers, MA, USA), total NF- κ B p65 (#4764, 1:1000; Cell Signaling Technology) and β -actin (#3700, 1:1000; Cell Signaling Technology), the membranes were washed with PBS three times. Subsequently, the membranes were incubated with horseradish peroxidase-conjugated secondary antibody. A total of 50 μ g of protein was used for western blotting analysis. The signals were detected by a chemiluminescence detection kit (GE Healthcare, Pittsburgh, PA, USA). The band intensity was quantified using Image-Pro Plus 6.0 software (Media Cybernetics, Inc, Rockville, MD, USA).

Statistical analysis

Results are presented as mean \pm standard deviation of at least three independent experiments. A two-tailed unpaired Student's t-test was performed for comparison between two groups. One-way

Table 1Murine primers for qRT-PCR.

Gene	Forward primer, 5'-3'	Reverse primer, 5′–3′
TNFA	TACTGAACTTCGGGGTGAT	CAGGCTTGTCACTCGAATT
IL1B	CAACCAACAAGTGATATTCTCC	GATCCACACTCTCCAGCTGCA
IL6	GTCAATTCCAGAAACCGCTATG	ACAGGTCTGTTGGGAGTGGT
IL10	AGGCAGCCTTGCAGAAAAGA	GCTCCACTGCCTTGCTCTTA
TLR4	AGCTTCTCCAATTTTTCAGAACTTC	TGAGAGGTGGTGTAAGCCATGC
PDCD4	ACTGACCCTGACAATTTAAGCG	TTTTCCGCAGTCGTCTTTTGG
CLTC	CTTTGGCACAGGGATAGGAAAT	GCTGATCTTTTTGCTTTCGGTT
ACTB	CATCCGTAAAGACCTCTATGCCAAC	ATGGAGCCACCGATCCACA-
U6	CTCGCTTCGGCAGCACA	AACGCTTCACGAATTTGCGT

ACTB, β -actin; CLTC, clathrin heavy chain.

6

analysis of variance was used to compare multiple groups. Kaplan—Meier analysis was used to estimate survival curves. P < 0.05 indicated statistical significance. All statistical analyses were performed using Prism 9 software (GraphPad Software, San Diego, CA, USA).

Results

Characterization of MSC sEVs

sEVs were obtained from the conditioned medium of mouse bone marrow-derived MSCs through ultracentrifugation. Transmission electron microscopy was used to observe the ultrastructure of MSC sEVs. Figure 1B displays the spheroid-shaped morphology of MSC sEVs, which ranged from 80 nm to 100 nm in size. Through nanoparticle tracking analysis, the authors measured the size distribution and number of sEVs. The mean diameter of sEVs was 88 \pm 42.3 nm (Figure 1D). The authors isolated 1.8 \times 10⁶ particles (containing 4.82 μg of sEV protein) from the culture medium of 1 \times 10⁶ MSCs (see supplementary Table 1). Western blotting analysis revealed the expression of CD81 and TSG101 proteins, but the endoplasmic reticulum marker calnexin was not expressed (Figure 1C).

MSC sEV treatment improved survival and attenuated organ injury in CLP-induced sepsis

The mouse treatment scheme is shown in Figure 2A. Kaplan—Meier survival curves showed that the survival rate of CLP mice treated with MSC sEVs was significantly higher than that of CLP mice treated with saline (60% in the CLP+MSC sEV group versus 30% in the CLP+saline group) (Figure 2B). This result indicated that MSC sEVs exerted protective effects against CLP-induced sepsis.

The number of CFUs in mouse peritoneal lavage fluid and blood was counted to assess bacterial burden (Figure 2C). Mice that received CLP surgery had a significantly larger number of CFUs in both peritoneal lavage fluid and blood than mice that received sham surgery (P < 0.05). However, CLP mice that received MSC sEV therapy exhibited a significantly lower number of CFUs in both peritoneal lavage fluid and blood than mice that received normal saline (P < 0.05), which indicated that MSC sEVs made direct or indirect contributions to bacterial clearance.

To analyze the effect of MSC sEVs on multi-organ dysfunction, the authors evaluated the pathology and function of the major organs (i. e., liver, pancreas, kidneys and lungs) of mice treated with or without MSC sEVs. The authors found that mice subjected to CLP showed more obvious dysfunction of the liver (as reflected by ALT, AST and bilirubin levels), pancreas (as reflected by amylase levels) and kidneys (as reflected by BUN and creatinine levels) than mice subjected to the sham operation (P < 0.01) (Figure 2D). However, when CLP mice were treated with MSC sEVs, their organ injuries were less severe compared with those administered saline (P < 0.01). Similarly, the pathological scores—which were used to evaluate edema, inflammatory cell infiltration and severe hemorrhage—in mice with the CLP operation were higher than the scores in mice receiving the sham operation. The pathological scores were also significantly reduced after treatment with MSC sEVs (P < 0.01) (Figure 2E).

MSC sEVs attenuated lung vascular permeability and inflammation in CLP-induced sepsis

The concentrations of total protein in BALF and lung wet:dry ratios were evaluated to assess pulmonary vascular leakage. CLP surgery significantly increased lung vascular permeability (P < 0.05 for total protein and P < 0.01 for lung wet:dry ratio compared with the sham group) (Figure 3A,B). Treatment with MSC sEVs markedly reversed the increase in lung vascular permeability in CLP mice (P < 0.05)

0.05 for total protein and P < 0.01 for lung wet:dry ratio compared with the CLP+saline group). Additionally, total cell counts in the BALF were detected to evaluate lung inflammation. The results revealed that both total cells and neutrophils in the BALF were significantly increased in the CLP+saline group compared with the sham group (P < 0.01). Treatment with MSC sEVs prevented this CLP-induced increase (P < 0.01) (Figure 3C,D).

MSC sEVs decreased plasma cytokine/chemokine levels in CLP-induced sepsis

Sepsis is characterized by a systemic inflammatory response. The authors measured the concentrations of plasma cytokines and chemokines that could reflect the systemic inflammatory response in CLP mice. The authors' results showed that levels of pro-inflammatory cytokines TNF- α , IL-1 β and IL-6 were significantly elevated in the plasma of mice that received CLP surgery compared with mice that received sham surgery (P < 0.01) (Figure 3E–H). However, administration of MSC sEVs significantly attenuated these increases (P < 0.01) (Figure 3E–G). Moreover, the anti-inflammatory cytokine IL-10 was significantly increased after treatment with MSC sEVs (P < 0.01) (Figure 3H).

The authors also detected the retention of MSC sEVs in lung tissues. At 6 h after administration, Dil-labeled MSC sEVs were observed in the perinuclear region of macrophages (anti-mouse F4/80-positive cells) (Figure 3I). The percentages of macrophages surrounded by Dillabeled MSC sEVs were significantly higher in CLP+sEV mice compared with sham+sEV mice (see supplementary Figure 2).

miR-21a-5p was abundantly expressed in MSC sEVs and could be delivered into BMDMs

A vast number of studies have demonstrated that MSC sEVs mediate cellular communication by shuttling miRNAs. Therefore, the authors selected a class of inflammation-related miRNAs (i.e., miR-125b, miR-27a, miR-21a, miR-93, miR-15a, miR-146a, miR-181b, miR-127, miR-130a, miR-106a, miR-106b, miR-126, miR-223) for the present study based on previous reports [33,34]. The authors performed qRT-PCR to analyze the differential expression of these miR-NAs in MSC sEVs. The results showed that miR-21a-5p was the most highly expressed miRNA among the inflammation-related miRNAs (Figure 4A). miR-21a has been reported to attenuate inflammation and to be protective against sepsis in several studies [35-37]. Therefore, the authors focused on MSC sEV miR-21a-5p for further investigation. To determine whether MSC sEVs could be internalized in BMDMs, Dil-labeled MSC sEVs were cultured for 24 h with BMDMs stimulated with 100 ng/mL LPS. The authors observed that Dillabeled MSC sEVs were internalized by BMDMs (Figure 4B). The authors further found that the expression of miR-21a-5p was markedly elevated in BMDMs after co-culturing with MSC sEVs for 24 h (P < 0.01) (Figure 4C). When the uptake of MSC sEVs by BMDMs was blocked, the expression of miR-21a-5p was significantly decreased (see supplementary Figure 3), which confirmed that increased miR-21a-5p in BMDMs was due to internalization of sEVs.

miR-21a-5p targeted TLR4 and PDCD4

Bioinformatics analysis with TargetScan predicted that miR-21a-5p targeted TLR4 and PDCD4 and indicated that the 3′ UTRs of TLR4 and PDCD4 were complementary to the miR-21a-5p seed region (Figure 4D). To validate that the 3′ UTRs of TLR4 and PDCD4 were direct targets of miR-21a-5p, the authors conducted dual-luciferase reporter gene assays. The luciferase activity of TLR4-wt and PDCD4-wt was reduced upon miR-21a mimic transfection, whereas the luciferase activity of TLR4-mut and PDCD4-mut was not changed (P < 0.01) (Figure 4E). Moreover, the RNA pull-down assay showed that

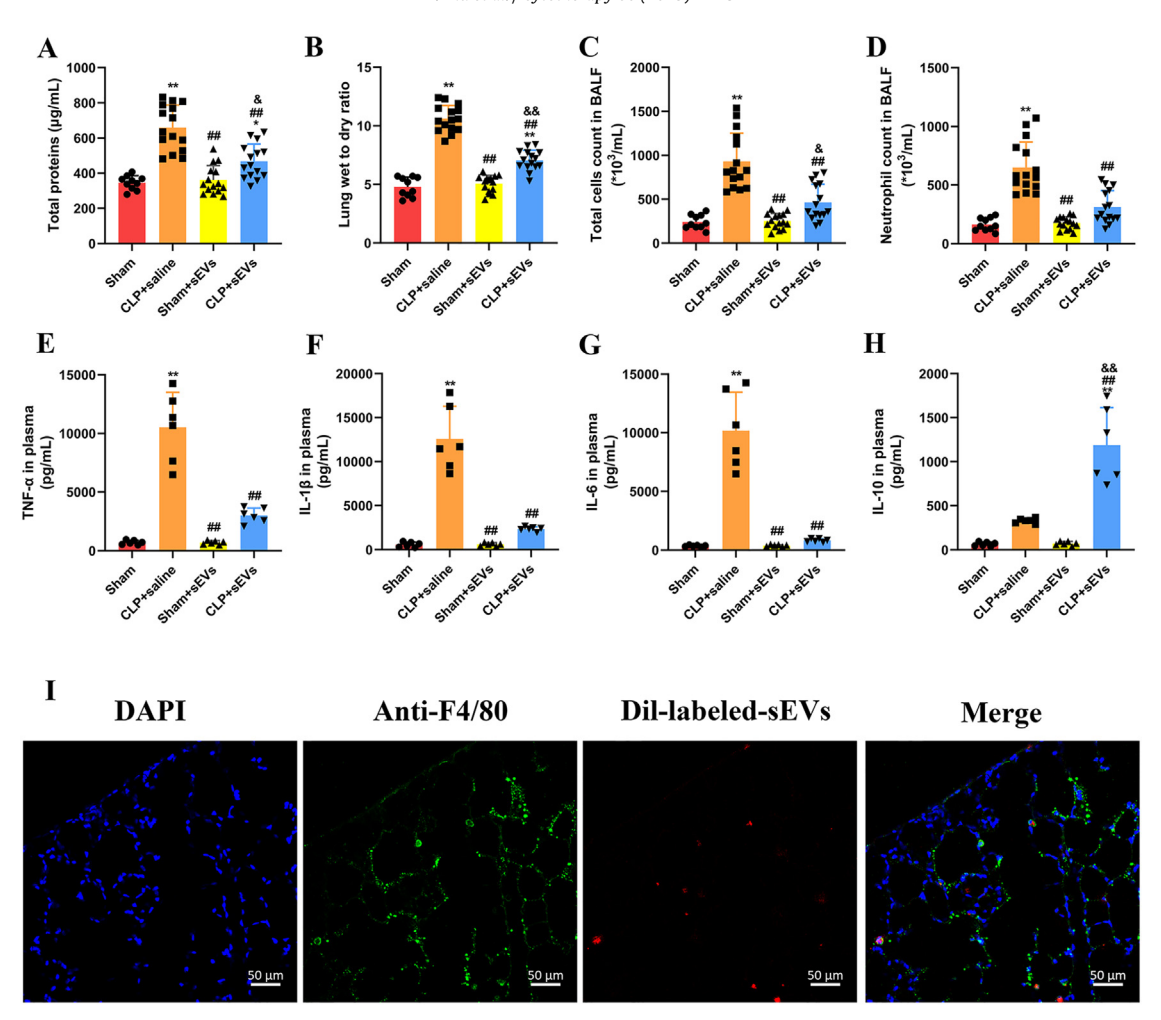


Fig. 3. MSC sEV treatment inhibits pulmonary microvascular permeability and plasma cytokine/chemokine levels in septic mice. (A,B) Pulmonary vascular permeability was assessed by measurement of (A) total protein in BALF and (B) lung wet:dry ratios (n = 15 for each group). (C,D) To evaluate lung inflammation, BALF was assessed for (C) total cell counts and (D) neutrophil counts (n = 15 for each group). (E–H) Plasma pro-inflammatory cytokines (E) TNF-α, (F) IL-1β and (G) IL-6 and the anti-inflammatory cytokine (H) IL-10 were measured by mouse ELISA (n = 15 for each group). (I) Representative images of MSC sEV incorporation in macrophages in lung tissues (n = 6 for each group) (scale bar = 50 μm). Statistical analysis was performed using one-way ANOVA with a Tukey–Kramer post-hoc test. Results are presented as mean ± SD. **P < 0.01, *P < 0.05, compared with the Sham group. ## P < 0.01, compared with the CLP+saline group, & P < 0.05, compared with the Sham+sEVs group. DAPI, 4',6-diamidino-2-phenylindole; ELISA, enzyme-linked immunosorbent assay; SD, standard deviation.

both TLR4 and PDCD4 were enriched with biotinylated miR-21a-3p, proving their direct interaction (P < 0.01) (Figure 4F). To prove that miR-21a-5p could specifically regulate the expression of TLR4 and PDCD4, the authors used miR-21a-5p mimics and inhibitors to transfect BMDMs. The level of miR-21a-5p was significantly increased after transfection of miR-21a-5p mimics, whereas it was significantly decreased after transfection of miR-21a-5p inhibitors (P < 0.01) (Figure 4I). The authors also found that miR-21a-5p mimics significantly reduced TLR4 and PDCD4 expression, whereas miR-21a-5p inhibitors led to elevation of TLR4 and PDCD4 expression (Figure 4G, H). Collectively, these data indicate that miR-21a-5p negatively regulated the expression of TLR4 and PDCD4 by binding to the 3' UTR.

MSC sEVs inhibited TLR4 and PDCD4 expression in BMDMs and lung tissues

The levels of miR-21a-5p target genes, including TLR4 and PDCD4, were markedly reduced at both the mRNA and protein levels in LPS-induced BMDMs after treatment with MSC sEVs (P < 0.01) (Figure 5A–D). A similar trend was observed in the protein level of phosphorylated NF- κ B p65, which is downstream of TLR4 and PDCD4 (P < 0.01) (Figure 5E). The data suggest that miR-21a-5p can be transferred into target cells to regulate gene expression.

Because MSC sEVs have been reported to accumulate mainly in the lungs, the authors specifically focused on lung tissues to explore the mechanisms of MSC sEVs in vivo. The results revealed that treatment with MSC sEVs significantly increased miR-21a-5p expression levels in lung tissues of mice that underwent CLP or sham operation (P < 0.05 for the sham+sEV group and P < 0.01 for the CLP+sEV group compared with the sham group) (Figure 5F). Moreover, MSC sEV therapy significantly reduced the mRNA and protein expression of both TLR4 and PDCD4—known targets of miR-21a-5p—in the lung tissues of septic mice (P < 0.01) (Figure 5G–J). Additionally, levels of phosphorylated NF- κ B p65 protein were significantly reduced in the lung tissues of septic mice after treatment with MSC sEVs (P < 0.01) (Figure 5K).

MSC sEVs suppressed inflammation in vitro and in vivo through the delivery of miR-21a-5p

To explore the effects of miR-21a-5p derived from MSC sEVs on sepsis *in vitro*, BMDMs were co-cultured with MSC sEVs that were additionally treated with miR-21a-5p inhibitor. LPS increased the mRNA and protein expression of pro-inflammatory cytokines TNF- α , IL-1 β and IL-6 (P < 0.01) as well as TLR4 and PDCD4 and the level of phosphorylated NF- κ B p65 protein in BMDMs, whereas co-treatment with MSC sEVs alleviated these

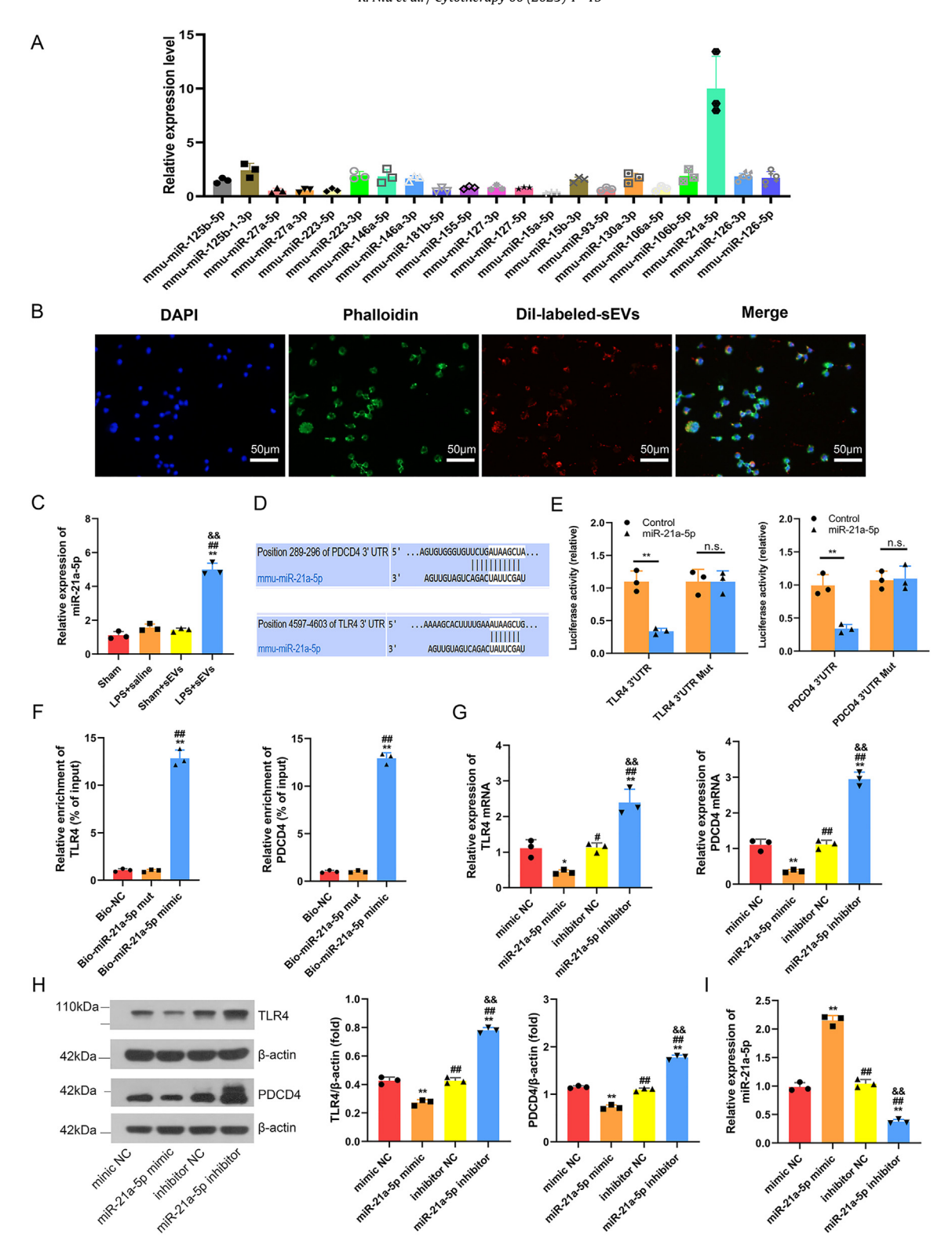


Fig. 4. miR-21a-5p targeted TLR4 and PDCD4. (A) Detection of expression of indicated miRNAs by qRT-PCR analysis (n = 3). (B) Fluorescence microscopy analysis of Dil-labeled MSC sEV internalization by BMDMs. Dil-labeled MSC sEVs (red) are visible in the perinuclear region of BMDMs (scale bar = 50 μm). (C) Levels of miR-21a-5p in LPS-stimulated BMDMs after co-culturing with or without MSC sEVs for 4 h (n = 3 per group). (D) Bioinformatics analysis with TargetScan predicts that the 3′ UTRs of TLR4 and PDCD4 are complementary to the miR-21a-5p seed region. (E) Luciferase activity of TLR4-wt and TLR4-mut or PDCD4-wt and PDCD4-mut was determined upon miR-21 mimic transfection (n = 3 per group). (F) Enrichment of miR-21a-5p detected by RNA pull-down assay in BMDMs. (G,H) mRNA and protein levels of TLR4 and PDCD4 in LPS-stimulated BMDMs after transfection with or without miR-21a-5p mimics or inhibitors (n = 3 per group). (I) Level of miR-21a-5p in LPS-stimulated BMDMs after transfection with or without miR-21a-5p mimics or inhibitors (n = 3 per group). Statistical analysis was performed using one-way ANOVA with a Tukey-Kramer post-hoc test. Results are presented as mean ± SD. For (C): ** P < 0.01, compared with the Sham group. ## P < 0.01, compared with the Bio-NC group. ## P < 0.01, compared with the Bio-miR-21a-5p mut group. For (G-I): ** P < 0.01, *P < 0.05, compared with the mimic NC group. ## P < 0.01, compared with the miR-21a-5p mimic group. &P < 0.01, compared with the inhibitor NC group.ANOVA, analysis of variance; DAPI, 4′,6-diamidino-2-phenylindole; SD, standard deviation.

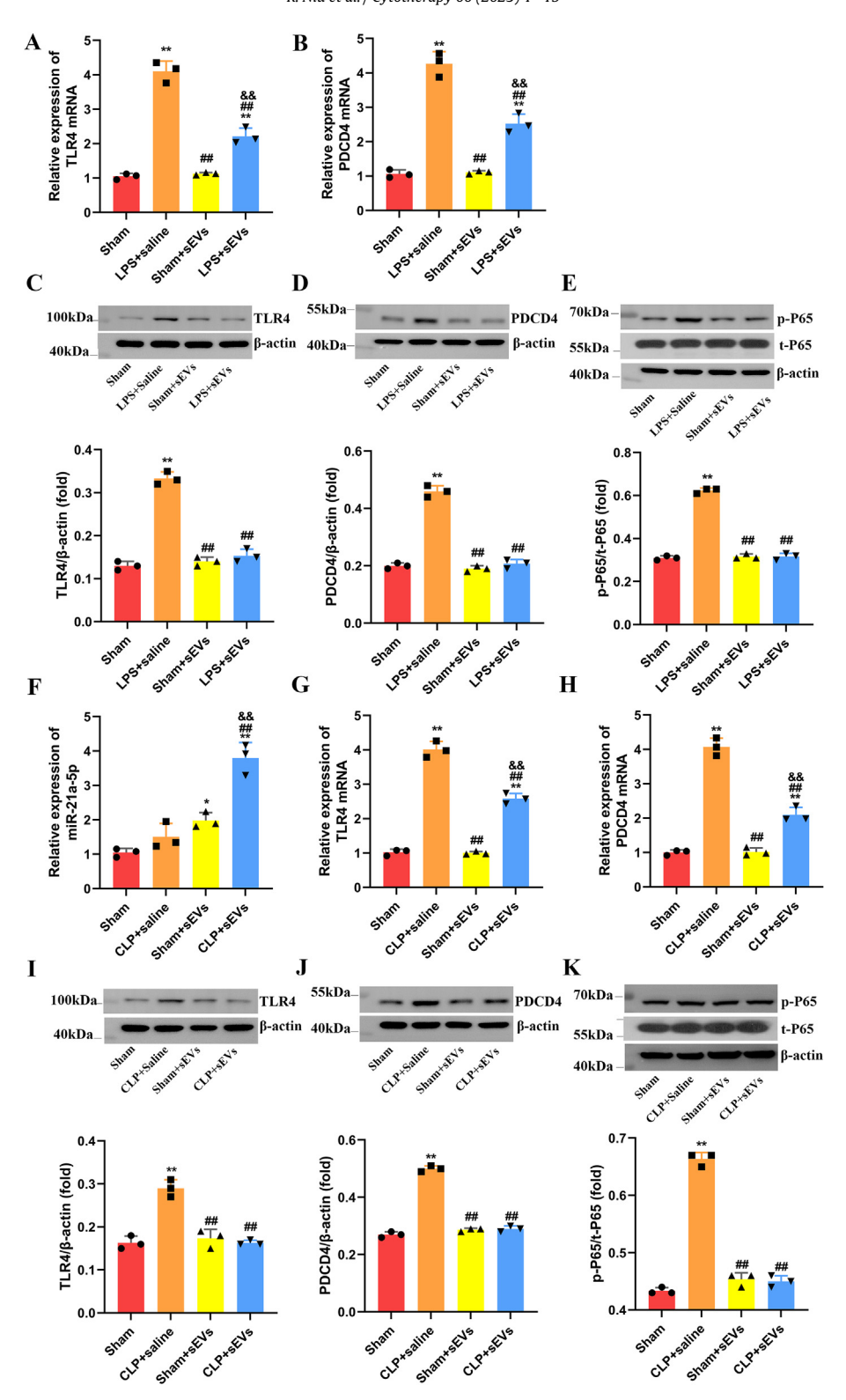


Fig. 5. miR-21a-5p targeted TLR4 and PDCD4 and inhibited their expression in BMDMs and lung tissues. (A–D) mRNA and protein levels of TLR4 and PDCD4 in LPS-stimulated BMDMs after co-culturing with or without MSC sEVs for 4 h. (E) Protein level of phosphorylated NF- κ B p65 in LPS-stimulated BMDMs after co-culturing with or without MSC sEVs for 4 h. (E) Protein level of (G) TLR4 and (H) PDCD4 in lung tissues of septic mice were determined with qRT-PCR. (I–K) Protein levels of (I) TLR4, (J) PDCD4 and (K) phosphorylated NF- κ B p65 in lung tissues of septic mice were measured by western blot. Statistical analysis was performed using one-way ANOVA with a Tukey—Kramer post-hoc test. Results are presented as mean \pm SD (n = 3 per group). For (A-E): ** P < 0.01, compared with the Sham group. ## P < 0.01, compared with the Sham+sEVs group. For (F-K): ** P < 0.01, ** P < 0.05, compared with the Sham group. ## P < 0.01, compared with the CLP+saline group. && P < 0.01, compared with the Sham+sEVs group. Results are represented as mean \pm SD. n = 3 per group. ANOVA, analysis of variance; SD, standard deviation.

effects (Figure 6A-M). MSC sEVs also significantly increased the anti-inflammatory cytokine IL-10 (P < 0.01) (Figure 6D,H). Moreover, inhibition of MSC sEV miR-21a-5p markedly reversed these

reductions in pro-inflammatory cytokines, TLR4, PDCD4 and phosphorylated NF- κ B p65 as well as the increase in anti-inflammatory cytokine IL-10 (Figure 6A–M).

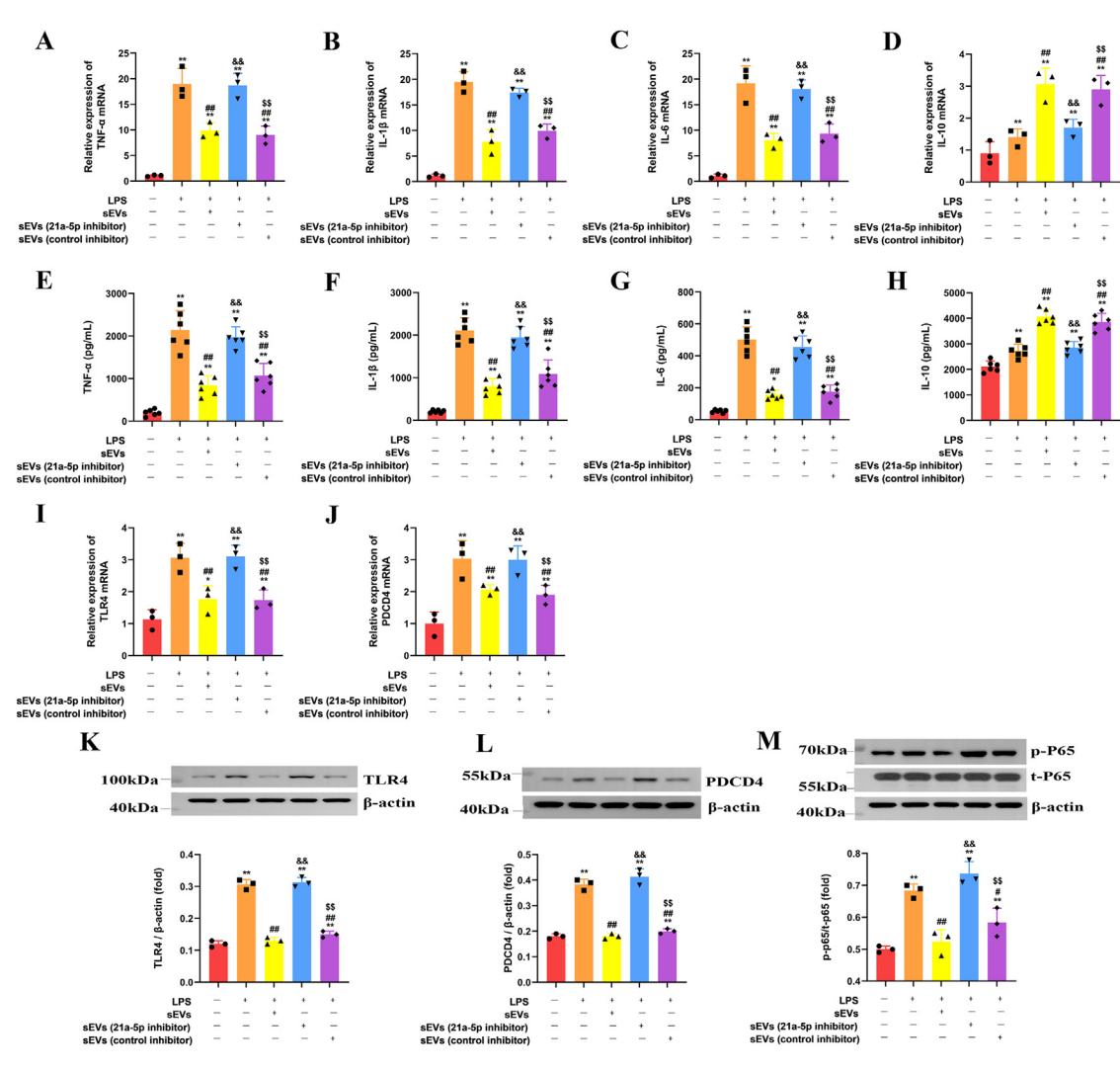


Fig. 6. MSC sEV treatment suppressed inflammation in BMDMs through the delivery of miR-21a-5p. BMDMs were co-cultured with MSC sEVs, which were additionally treated with a specific inhibitor targeting miR-21a-5p. (A–H) mRNA and protein expression of pro-inflammatory cytokines (A,E) TNF- α , (B,F) IL-1 β and (C,G) IL-6 and anti-inflammatory cytokine (D,H) IL-10 in BMDMs was determined by qRT-PCR and mouse ELISA, respectively (n = 3 per group). (I,J) mRNA expression of (I) TLR4 and (J) PDCD4 in BMDMs was determined by qRT-PCR (n = 6 per group). (K–M) Protein levels of (K) TLR4, (L) PDCD4 and (M) phosphorylated NF- α B post in BMDMs were measured by western blot (n = 3 per group). Statistical analysis was performed using one-way ANOVA with a Tukey–Kramer post-hoc test. Results are presented as mean ± SD. ** P < 0.01, * P < 0.05, compared with the Sham group. ## P < 0.01, compared with the LPS+seline group. \$\$ P < 0.01, compared with the LPS+selvs (21a-5p inhibitor) group. ANOVA, analysis of variance; ELISA, enzyme-linked immunosor-bent assay; SD, standard deviation.

Similar trends were observed *in vivo* for the mRNA and protein expression of TLR4 and PDCD4 and the protein expression of phosphorylated NF- κ B p65 in the lung tissues of septic mice (P < 0.01) (Figure 7B–F). Additionally, the authors explored the potential effect of miR-21a-5p derived from MSC sEVs on the survival rate of septic mice. MSC sEV administration significantly increased the survival rate of CLP mice compared with mice administered saline (P < 0.05) (Figure 7A). However, there were no significant differences in the survival rate between CLP mice administered miR-21a-5p-depleted MSC sEVs and CLP mice administered saline (P > 0.05). These data suggest that MSC sEVs suppressed inflammation by targeting TLR4 and PDCD4 through miR-21a-5p.

Inhibition of TLR4 and PDCD4 induced MSC sEV-like positive effects on BMDMs

The authors additionally tested whether inhibiting the expression of miR-21a-5p target genes TLR4 and PDCD4 had similar beneficial effects on BMDMs as MSC sEVs. The authors' data showed that the most effective siRNAs were siTLR4 #1 and siPDCD4 #1, both of which were selected for subsequent experiments (P < 0.01) (Figure 8A,B).

The authors then found that inhibition of TLR4 and PDCD4 significantly reduced the mRNA and protein expression of pro-inflammatory cytokines TNF- α , IL-1 β and IL-6 and increased the expression of anti-inflammatory cytokine IL-10 in LPS-stimulated BMDMs (P < 0.01) (Figure 8C–J). The beneficial effects on BMDMs induced by siTLR4 #1 and siPDCD4 #1 were almost the same as those induced by treatment with MSC sEVs (P < 0.01), which further indicated that the beneficial effects of MSC sEVs on BMDMs may be in part mediated through miR-21a-5p targeting of TLR4 and PDCD4. Moreover, TLR4 signaling inhibitor (TAK-242) treatment were also observed the similar anti-inflammatory effect on BMDMs with siTLR4 (see supplementary Figure 4).

MSC sEVs suppressed inflammation in vitro through the miR-21a-5p-TLR4/PDCD4 pathway

To investigate the regulatory role of miR-21a-5p in sepsis, the authors introduced miR-21a-5p mimic-transfected MSC sEVs along with TLR4 and PDCD4 overexpression lentiviral particles into BMDMs. The authors' qRT-PCR and western blot analysis showed that miR-21a-5p mimic-transfected MSC sEVs significantly

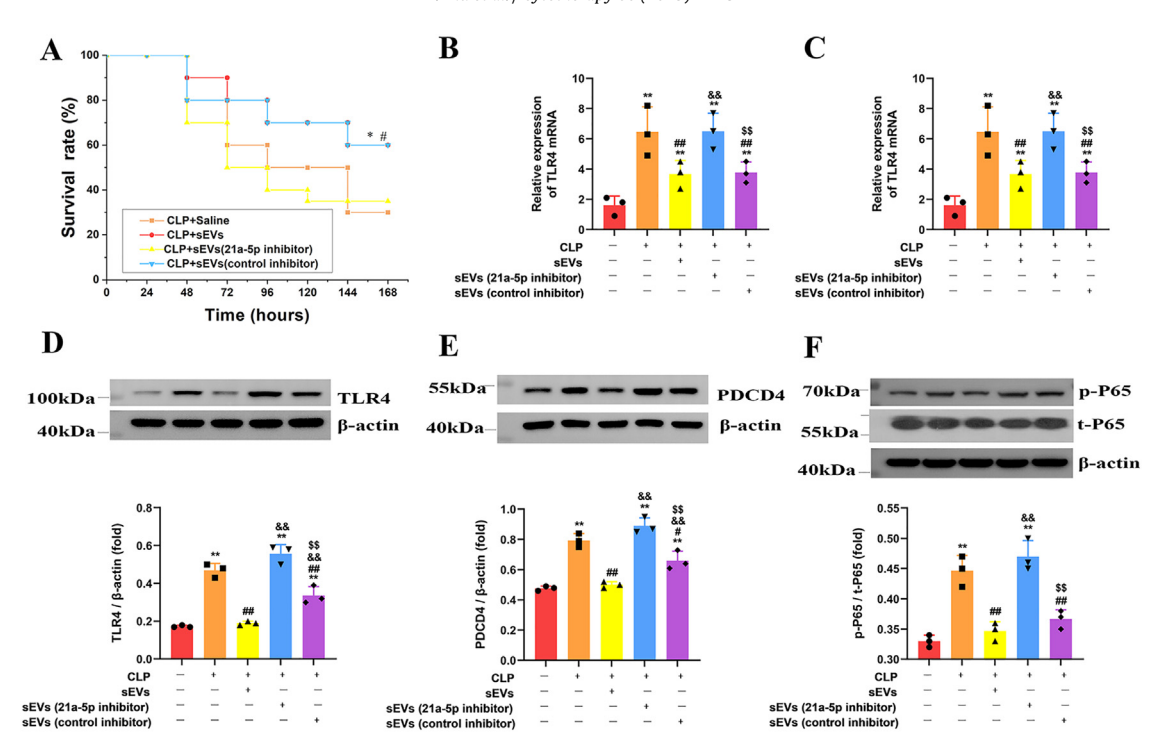


Fig. 7. MSC sEV treatment suppressed inflammation in lung tissues of septic mice through the delivery of miR-21a-5p. CLP-induced septic mice were treated with saline, MSC sEVs or miR-21a-5p-depleted MSC sEVs. (A) Survival rate in CLP mice was monitored for a total of 168 h (7 days) (n = 20 per group). (B,C) mRNA expression of (B) TLR4 and (C) PDCD4 in lung tissues of septic mice was determined by qRT-PCR (n = 3 per group). (D-F) Protein expression of (D) TLR4, (E) PDCD4 and (F) phosphorylated NF- κ B p65 in lung tissues of septic mice was determined by western blot (n = 3 per group). Statistical analysis was performed using one-way ANOVA with a Tukey-Kramer post-hoc test. Results are presented as mean \pm SD. For (A) *P < 0.05, CLP+sEVs group or CLP+ sEVs (control inhibitor) compared with the CLP+selvis (21a-5p inhibitor). For (B-F), ** P < 0.01, compared with the CLP+sEVs group. \$\$ P < 0.01, compared with the CLP+sEVs group. \$\$ P < 0.01, compared with the CLP+sEVs group. \$\$ P < 0.01, compared with the CLP+sEVs (21a-5p inhibitor) group. ANOVA, analysis of variance; SD, standard deviation.

downregulated TLR4 and PDCD4 expression. However, when BMDMs were infected with TLR4 or PDCD4 overexpression lentivirus, the benefit effect of miR-21a-5p mimic-transfected MSC sEVs was reversed (Figure 9I–L). Moreover, functional analysis demonstrated that miR-21a-5p mimic-transfected MSC sEVs significantly reduced the expression of pro-inflammatory cytokines TNF- α , IL-1 β and IL-6 and increased the expression of anti-inflammatory cytokine IL-10. However, overexpression of TLR4 and PDCD4 reversed this change (Figure 9A–F). Collectively, these results reveal that MSC sEVs suppressed inflammation *in vitro* through the miR-21a-5p-TLR4/PDCD4 pathway.

Discussion

In this study, the authors explored the role of MSC sEVs in sepsis *in vitro* and *in vivo*. The authors proved that MSC sEVs significantly alleviate the symptoms of sepsis, including elevating survival rates and bacterial clearance, inhibiting lung vascular leakage and the inflammatory response and improving organ dysfunction. The authors found that the potential mechanisms underlying the beneficial effects of MSC sEVs on sepsis might be related to the delivery of miRNA. Moreover, the authors found that miR-21a-5p was highly abundant in MSC sEVs, could be delivered into recipient cells and targeted TLR4 and PDCD4.

Over the past decade, multiple studies have demonstrated that systemic injection of MSCs attenuates the inflammatory response and organ failure in several pre-clinical models of sepsis [5–7]. MSCs have additionally been confirmed to have beneficial effects on sepsis in early-phase clinical trials [8,9]. However, the utilization of MSCs as therapeutic agents for sepsis may be limited by technical challenges, including scaling up and maintaining the activities of stem cells. Recently, there has been increasing interest in using MSC sEVs in sepsis as an alternative to cell therapy [20]. MSC sEVs could provide

benefits to injured cells similar to MSCs themselves but avoid phagocytosis, degradation and modification in the circulation [38,39]. In the present study, sEVs derived from mouse MSCs improved murine survival, attenuated organ injury, reduced systemic inflammation and decreased lung vascular leakage in septic mice. Consistent with the authors' report, several studies have proven the beneficial effects of MSC- or endothelial progenitor cell-derived sEVs on septic mice [21,35,39]. The authors also observed that MSC sEVs had a minimal impact on pancreatic function compared with other organs based on amylase activity. This interesting observation may be related to the inhibition of inflammation and pyroptosis of pancreatic acinar cells [40] and the control of the systemic inflammatory response to facilitate the repair of pancreatic tissue by MSC sEVs [41]. A similar observation was also reported by Li *et al.* [40], who showed that MSC sEVs could alleviate inflammation and pyroptosis of pancreatic acinar cells.

The mechanisms related to the protective effects of MSC sEVs against sepsis have not been well characterized. Although there are numerous bioactive molecules in sEVs, reports have indicated that miRNAs might play a critical role in the beneficial effects of sEVs on recipient cells [34,42]. sEVs are considered vehicles for the horizontal transfer of miRNAs between cells to regulate gene expression and biological processes [43,44]. miR-21 has been demonstrated to be present in sEVs derived from several kinds of cells, including cancerassociated adipocytes and fibroblasts [45], dendritic cells [46], bronchial epithelial cells [47], endothelial progenitor cells [37,48] and human umbilical cord blood cells [49]. The results of the current study showed that high levels of miR-21a-5p were identified in sEVs derived from mouse bone marrow MSCs. Moreover, miR-21a-5p expression was markedly enhanced in both BMDMs incubated with MSC sEVs and lung tissues of septic mice that received MSC sEV therapy. The data suggest that miR-21a-5p can be transferred from MSC sEVs to target cells.

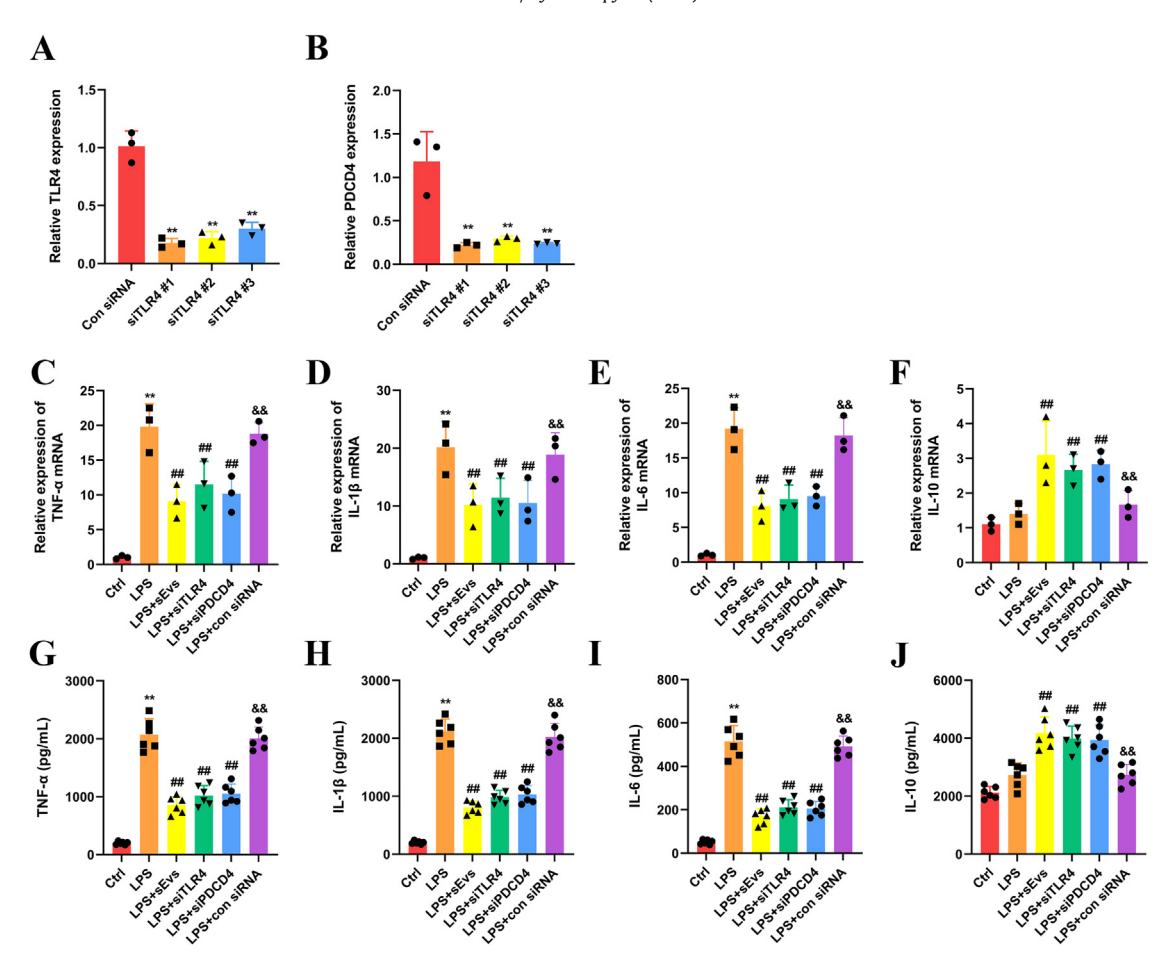


Fig. 8. Inhibition of TLR4 and PDCD4 induced MSC sEV-like positive effects on BMDMs. BMDMs were co-cultured with MSC sEVs, siTLR4 or siPDCD4. (A,B) Inhibitory efficiency of siRNAs targeting (A) TLR4 and (B) PDCD4 was verified by qRT-PCR (n = 3 per group). (C–J) mRNA and protein expression of pro-inflammatory cytokines (C,G) TNF-α, (D,H) IL-1β and (E,I) IL-6 and anti-inflammatory cytokine (F,J) IL-10 in BMDMs was determined by qRT-PCR and mouse ELISA, respectively (n = 3 per group for mRNA and n = 6 per group for protein). Statistical analysis was performed using one-way ANOVA with a Tukey–Kramer post-hoc test. Results are presented as mean \pm SD. For (A) and (B), ** P < 0.01, compared with the Con siRNA group. For (C–J), ** P < 0.01, compared with the control group. ## P < 0.01, compared with the LPS+saline group. && P < 0.01. ANOVA, analysis of variance; Con siRNA, negative control siRNA; Ctrl, control; ELISA, enzyme-linked immunosorbent assay; SD, standard deviation, compared with the LPS+sEVs group.

Growing evidence has revealed that miR-21 performs a pivotal function in inflammatory responses [36,50–52]. The importance of miR-21a-5p in sepsis has been demonstrated in CLP-induced acute kidney injury mouse models that have high renal tubular injury scores, inflammatory factor levels and oxidative stress responses [37,53]. Through its targeting of TLR4, miR-21a-5p regulates inflammatory responses in *Mycobacterium tuberculosis*-infected macrophages [54] and LPS-stimulated NR8383 cells [36]. Additionally, miR-21 has been demonstrated to target and inhibit PDCD4, a selective protein translation inhibitor known to inhibit inflammation and a proposed target for sepsis therapeutics [35]. More recently, reports have shown that the miR-21-dependent regulation of inflammation in sepsis is mediated by NF-κB p65 phosphorylation [53].

In summary, this study revealed that the expression levels of TLR4, PDCD4 and phosphorylated NF- κ B p65 were significantly decreased in BMDMs and CLP-induced septic mice treated with miR-21-5p-containing MSC sEVs. However, the positive roles played by MSC sEVs were significantly reversed by a specific inhibitor targeting miR-21-5p. Moreover, the authors found that knocking down the expression of miR-21-5p target genes TLR4 and PDCD4 could provide MSC sEV-like protective effects with regard to the inflammatory response in BMDMs. These findings indicate that miR-21-5p transferred by MSC sEVs might provide an anti-inflammatory benefit in sepsis by targeting TLR4 and PDCD4.

Several limitations of this study should be pointed out. First, a great number of bioactive molecules were identified in MSC sEVs, and the authors focused on only miRNAs in this work. The authors cannot exclude the possibility that other bioactive molecules within MSC sEVs contribute to the beneficial effects against sepsis; this requires further exploration. Second, the results of the authors' study revealed that miR-21a-5p accounts for a portion of the therapeutic effects of MSC sEVs in sepsis. However, the possibility that other MSC sEV miRNAs may also play a role in sepsis therapy cannot be excluded. Ongoing research involving bioinformatics analysis may detect additional miRNAs in MSC sEVs that are related to sepsis. Third, miRNA regulation is a network system: miRNAs may be regulated by other molecules and miRNAs may regulate different targets as well. Further mechanistic studies to explore the therapeutic effect of MSC sEV miR-21a-5p in sepsis are still needed.

Conclusions

In summary, the authors' present data indicate that sEVs released from MSCs improve survival and attenuate organ injury in septic mice through the inhibition of inflammation. Moreover, the authors' results reveal that the mechanisms underlying the protective effects of MSC sEVs against sepsis might be related to the delivery of miR-21a-5p. More importantly, MSC sEV-derived miR-21a-5p is likely to suppress inflammation by targeting TLR4 and PDCD4 (Figure 10).

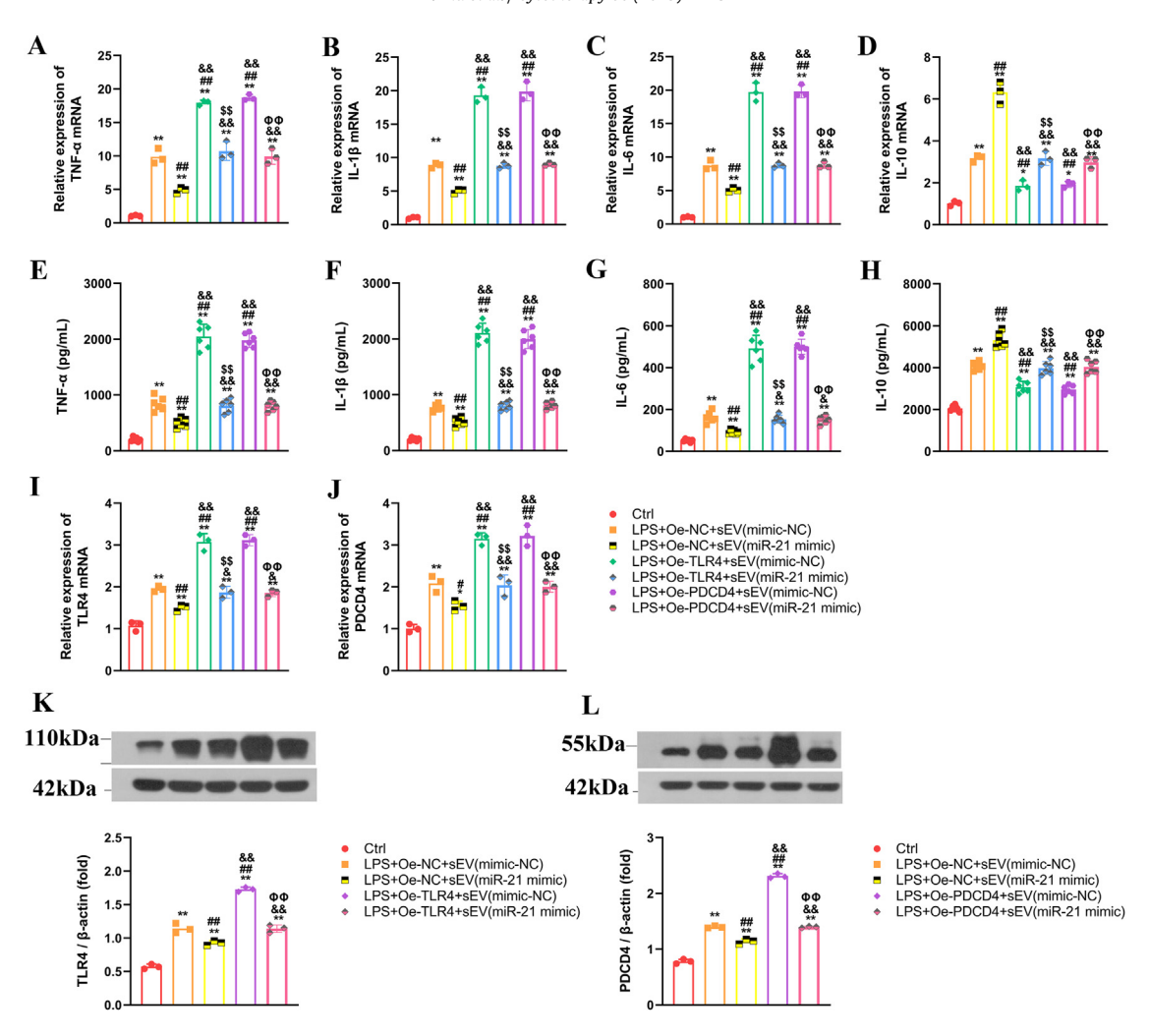


Fig. 9. MSC sEVs suppressed inflammation *in vitro* through the miR-21a-5p-TLR4/PDCD4 pathway. miR-21a-5p mimic-transfected MSC sEVs along with TLR4 and PDCD4 overexpression lentiviral particles were transfected into BMDMs. (A–H) mRNA and protein expression of pro-inflammatory cytokines (A,E) TNF- α , (B,F) IL-1 β and (C,G) IL-6 and anti-inflammatory cytokine (D,H) IL-10 in BMDMs was determined by qRT-PCR and mouse ELISA, respectively (n = 3 per group). (I–L) mRNA expression of (I,K) TLR4 and (J,L) PDCD4 in BMDMs was determined by qRT-PCR and western blot, respectively (n = 3 per group). Statistical analysis was performed using one-way ANOVA with a Tukey–Kramer post-hoc test. Results are presented as mean ± SD. Statistical analysis: one-way ANOVA with a Tukey–Kramer post hoc test. ** P < 0.01, *P < 0.05, compared with the LPS+Oe-NC+sEV(mimic-NC) group; &P < 0.01, &P < 0.05, compared with the LPS+Oe-NC+sEV(mimic-NC) group; &P < 0.01, compared with the LPS+Oe-TLR4+sEV(mimic-NC) group; $\Phi\Phi$ P < 0.01, compared with the LPS+Oe-PDCD4+sEV(mimic-NC) group; ELISA, enzyme-linked immunosorbent assay.

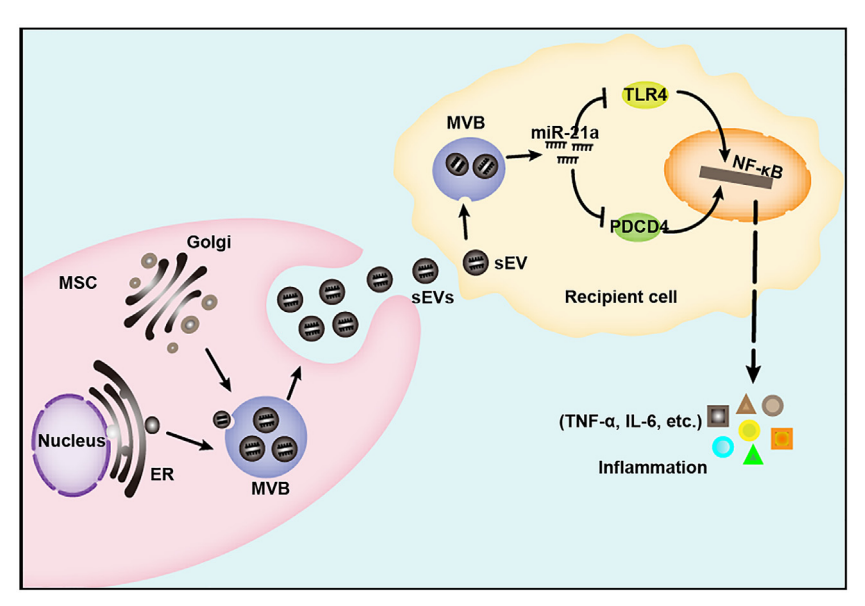


Fig. 10. Schematic illustration of the mechanism of MSC sEVs in the treatment of sepsis. MSC sEVs inhibited sepsis-associated inflammation through the delivery of miR-21a-5p. Moreover, MSC sEV-derived miR-21a-5p is likely to suppress inflammation by targeting TLR4 and PDCD4. ER, endoplasmic reticulum; MVB, multivesicular body.

Ongoing investigation into the role of MSC sEVs will allow us to better understand their potential as novel sepsis therapeutics.

Declaration of Competing Interest

The authors have no commercial, proprietary or financial interest in the products or companies described in this article.

Funding

The present study was supported by the Natural Science Foundation of Xinjiang Uygur Autonomous Region (2022D01C498), China Postdoctoral Science Foundation (2022M713520), National Natural Science Foundation of China (81600063), Natural Science Foundation of Hunan Province (2017JJ3484) and State Key Laboratory Program (SKLKF 201903).

Author Contributions

Conception and design of the study: JC, RN, CL, and PP. Acquisition of data: JC, BL, HM, HH, ZZ, HY, SM, and FZ. Analysis and interpretation of data: JC, RN, BL, HM, HH, ZZ, HY, SM, and FZ. Drafting or revising the manuscript: JC, RN, and PP. All authors have approved the final article.

Data Availability

The datasets generated and analyzed for this study are available from the corresponding author upon reasonable request.

Supplementary materials

Supplementary material associated with this article can be found in the online version at doi:10.1016/j.jcyt.2023.02.002.

References

- [1] Freund Y, Lemachatti N, Krastinova E, Van Laer M, Claessens YE, Avondo A, Occelli C, Feral-Pierssens AL, Truchot J, Ortega M, Carneiro B, Pernet J, Claret PG, Dami F, Bloom B, Riou B, Beaune S. Prognostic Accuracy of Sepsis-3 Criteria for In-Hospital Mortality Among Patients With Suspected Infection Presenting to the Emergency Department. JAMA 2017;317:301–8.
- [2] Prescott HC, Angus DC. Enhancing Recovery From Sepsis: A Review. JAMA 2018;319:62–75.
- [3] Singer M, Deutschman CS, Seymour CW, Shankar-Hari M, Annane D, Bauer M, Bellomo R, Bernard GR, Chiche JD, Coopersmith CM, Hotchkiss RS, Levy MM, Marshall JC, Martin GS, Opal SM, Rubenfeld GD, van der Poll T, Vincent JL, Angus DC. The Third International Consensus Definitions for Sepsis and Septic Shock (Sepsis-3). JAMA 2016;315:801–10.
- [4] Fleischmann C, Scherag A, Adhikari NK, Hartog CS, Tsaganos T, Schlattmann P, Angus DC, Reinhart K. Assessment of Global Incidence and Mortality of Hospitaltreated Sepsis. Current Estimates and Limitations. Am J Respir Crit Care Med 2016;193:259–72.
- [5] Németh K, Leelahavanichkul A, Yuen PS, Mayer B, Parmelee A, Doi K, Robey PG, Leelahavanichkul K, Koller BH, Brown JM, Hu X, Jelinek I, Star RA, Mezey E. Bone marrow stromal cells attenuate sepsis via prostaglandin E(2)-dependent reprogramming of host macrophages to increase their interleukin-10 production. Nature medicine 2009:15:42-9
- [6] Hall SR, Tsoyi K, Ith B, Padera Jr. RF, Lederer JA, Wang Z, Liu X, Perrella MA. Mesenchymal stromal cells improve survival during sepsis in the absence of heme oxygenase-1: the importance of neutrophils. Stem cells (Dayton, Ohio) 2013;31:397–407.
- [7] Lombardo E, van der Poll T, DelaRosa O, Dalemans W. Mesenchymal stem cells as a therapeutic tool to treat sepsis. World journal of stem cells 2015;7:368–79.
- [8] Wilson JG, Liu KD, Zhuo H, Caballero L, McMillan M, Fang X, Cosgrove K, Vojnik R, Calfee CS, Lee JW, Rogers AJ, Levitt J, Wiener-Kronish J, Bajwa EK, Leavitt A, McKenna D, Thompson BT, Matthay MA. Mesenchymal stem (stromal) cells for treatment of ARDS: a phase 1 clinical trial. Lancet Respir Med 2015;3:24–32.
- [9] Galstian GM, Parovichnikova EN, Makarova PM, Kuzmina LA, Troitskaya VV, Gemdzhian E, Drize NI, Savchenko VG. The Results of the Russian Clinical Trial of Mesenchymal Stromal Cells (MSCs) in Severe Neutropenic Patients (pts) with Septic Shock (SS) (RUMCESS trial). Blood 2015;126:2220.
- [10] Phinney DG, Pittenger MF. Concise Review: MSC-Derived Exosomes for Cell-Free Therapy. Stem cells (Dayton, Ohio) 2017;35:851–8.

- [11] Allan D, Tieu A, Lalu M, Burger D. Mesenchymal stromal cell-derived extracellular vesicles for regenerative therapy and immune modulation: Progress and challenges toward clinical application. Stem cells translational medicine 2020;9:39–46.
- [12] Chen J, Li Y, Hao H, Li C, Du Y, Hu Y, Li J, Liang Z, Li C, Liu J, Chen L. Mesenchymal Stem Cell Conditioned Medium Promotes Proliferation and Migration of Alveolar Epithelial Cells under Septic Conditions *In Vitro* via the JNK-P38 Signaling Pathway. Cellular physiology and biochemistry: international journal of experimental cellular physiology, biochemistry, and pharmacology 2015;37:1830–46.
- [13] Su VY, Lin CS, Hung SC, Yang KY. Mesenchymal stem cell-conditioned medium induces neutrophil apoptosis associated with inhibition of the NF-κB pathway in endotoxin-induced acute lung injury. Int J Mol Sci 2019;20:2208. https://doi.org/ 10.3390/ijms20092208.
- [14] Zhou Y, Xu H, Xu W, Wang B, Wu H, Tao Y, Zhang B, Wang M, Mao F, Yan Y, Gao S, Gu H, Zhu W, Qian H. Exosomes released by human umbilical cord mesenchymal stem cells protect against cisplatin-induced renal oxidative stress and apoptosis *in vivo* and *in vitro*. Stem cell research & therapy 2013;4:34.
- [15] Wang B, Jia H, Zhang B, Wang J, Ji C, Zhu X, Yan Y, Yin L, Yu J, Qian H, Xu W. Preincubation with hucMSC-exosomes prevents cisplatin-induced nephrotoxicity by activating autophagy. Stem cell research & therapy 2017;8:75.
- [16] Lee C, Mitsialis SA, Aslam M, Vitali SH, Vergadi E, Konstantinou G, Sdrimas K, Fernandez-Gonzalez A, Kourembanas S. Exosomes mediate the cytoprotective action of mesenchymal stromal cells on hypoxia-induced pulmonary hypertension. Circulation 2012;126:2601–11.
- [17] Bian S, Zhang L, Duan L, Wang X, Min Y, Yu H. Extracellular vesicles derived from human bone marrow mesenchymal stem cells promote angiogenesis in a rat myocardial infarction model. Journal of molecular medicine (Berlin, Germany) 2014;92:387–97.
- [18] Tieu A, Lalu MM, Slobodian M, Gnyra C, Fergusson DA, Montroy J, Burger D, Stewart DJ, Allan DS. An Analysis of Mesenchymal Stem Cell-Derived Extracellular Vesicles for Preclinical Use. ACS nano 2020;14:9728–43.
- [19] Théry C, Witwer KW, Aikawa E, Alcaraz MJ, Anderson JD, Andriantsitohaina R, et al. Minimal information for studies of extracellular vesicles 2018 (MISEV2018): a position statement of the International Society for Extracellular Vesicles and update of the MISEV2014 guidelines. Journal of extracellular vesicles 2018;7:1535750.
- [20] Cheng Y, Cao X, Qin L. Mesenchymal Stem Cell-Derived Extracellular Vesicles: A Novel Cell-Free Therapy for Sepsis. Frontiers in immunology 2020;11:647.
- [21] Song Y, Dou H, Li X, Zhao X, Li Y, Liu D, Ji J, Liu F, Ding L, Ni Y, Hou Y. Exosomal miR-146a Contributes to the Enhanced Therapeutic Efficacy of Interleukin-1β-Primed Mesenchymal Stem Cells Against Sepsis. Stem cells (Dayton, Ohio) 2017;35:1208-21.
- [22] Tang XD, Shi L, Monsel A, Li XY, Zhu HL, Zhu YG, Qu JM. Mesenchymal Stem Cell Microvesicles Attenuate Acute Lung Injury in Mice Partly Mediated by Ang-1 mRNA. Stem cells (Dayton, Ohio) 2017;35:1849–59.
- [23] Phinney DG, Di Giuseppe M, Njah J, Sala E, Shiva S, St Croix CM, Stolz DB, Watkins SC, Di YP, Leikauf GD, Kolls J, Riches DW, Deiuliis G, Kaminski N, Boregowda SV, McKenna DH, Ortiz LA. Mesenchymal stem cells use extracellular vesicles to outsource mitophagy and shuttle microRNAs. Nature communications 2015;6:8472.
- [24] Collino F, Bruno S, Incarnato D, Dettori D, Neri F, Provero P, Pomatto M, Oliviero S, Tetta C, Quesenberry PJ, Camussi G. AKI Recovery Induced by Mesenchymal Stromal Cell-Derived Extracellular Vesicles Carrying MicroRNAs. Journal of the American Society of Nephrology: JASN 2015;26:2349–60.
- [25] Wang X, Gu H, Qin D, Yang L, Huang W, Essandoh K, Wang Y, Caldwell CC, Peng T, Zingarelli B, Fan GC. Exosomal miR-223 Contributes to Mesenchymal Stem Cell-Elicited Cardioprotection in Polymicrobial Sepsis. Scientific reports 2015; 5:13721.
- [26] Yu B, Kim HW, Gong M, Wang J, Millard RW, Wang Y, Ashraf M, Xu M. Exosomes secreted from GATA-4 overexpressing mesenchymal stem cells serve as a reservoir of anti-apoptotic microRNAs for cardioprotection. International journal of cardiology 2015;182:349–60.
- [27] Nong K, Wang W, Niu X, Hu B, Ma C, Bai Y, Wu B, Wang Y, Ai K. Hepatoprotective effect of exosomes from human-induced pluripotent stem cell-derived mesenchymal stromal cells against hepatic ischemia-reperfusion injury in rats. Cytotherapy 2016;18:1548–59.
- [28] Chen J, Li C, Gao X, Li C, Liang Z, Yu L, Li Y, Xiao X, Chen L. Keratinocyte growth factor gene delivery via mesenchymal stem cells protects against lipopolysaccharide-induced acute lung injury in mice. PLoS One 2013;8:e83303.
- [29] Théry C, Amigorena S, Raposo G, Clayton A. Isolation and characterization of exosomes from cell culture supernatants and biological fluids. Curr Protoc Cell Biol 2006; Chapter 3: Unit 3.22.
- [30] Li H, Wang S, Zhan B, He W, Chu L, Qiu D, Li N, Wan Y, Zhang H, Chen X, Fang Q, Shen J, Yang X. Therapeutic effect of Schistosoma japonicum cystatin on bacterial sepsis in mice. Parasites & vectors 2017;10:222.
- [31] Wan Z, Zhao L, Lu F, Gao X, Dong Y, Zhao Y, Wei M, Yang G, Xing C, Liu L. Mononuclear phagocyte system blockade improves therapeutic exosome delivery to the myocardium. Theranostics 2020;10:218–30.
- [32] Yeh CH, Yang JJ, Yang ML, Li YC, Kuan YH. Rutin decreases lipopolysaccharide-induced acute lung injury via inhibition of oxidative stress and the MAPK-NF-κB pathway. Free radical biology & medicine 2014;69:249–57.
 [33] Li JJ, Wang B, Kodali MC, Chen C, Kim E, Patters BJ, Lan L, Kumar S, Wang X, Yue J,
- [33] Li JJ, Wang B, Kodali MC, Chen C, Kim E, Patters BJ, Lan L, Kumar S, Wang X, Yue J, Liao FF. In vivo evidence for the contribution of peripheral circulating inflammatory exosomes to neuroinflammation. Journal of neuroinflammation 2018;15:8.
- [34] Poon KS, Palanisamy K, Chang SS, Sun KT, Chen KB, Li PC, Lin TC, Li CY. Plasma exosomal miR-223 expression regulates inflammatory responses during cardiac surgery with cardiopulmonary bypass. Scientific reports 2017;7:10807.

- [35] Yao M, Cui B, Zhang W, Ma W, Zhao G, Xing L. Exosomal miR-21 secreted by IL- 1β -primed-mesenchymal stem cells induces macrophage M2 polarization and ameliorates sepsis. Life sciences 2021;264:118658.
- [36] Zhu WD, Xu J, Zhang M, Zhu TM, Zhang YH, Sun K. MicroRNA-21 inhibits lipopoly-saccharide-induced acute lung injury by targeting nuclear factor-κB. Experimental and therapeutic medicine 2018;16:4616–22.
- [37] Zhang Y, Huang H, Liu W, Liu S, Wang XY, Diao ZL, Zhang AH, Guo W, Han X, Dong X, Katilov O. Endothelial progenitor cells-derived exosomal microRNA-21-5p alleviates sepsis-induced acute kidney injury by inhibiting RUNX1 expression. Cell death & disease 2021;12:335.
- [38] Laulagnier K, Motta C, Hamdi S, Roy S, Fauvelle F, Pageaux JF, Kobayashi T, Salles JP, Perret B, Bonnerot C, Record M. Mast cell- and dendritic cell-derived exosomes display a specific lipid composition and an unusual membrane organization. The Biochemical journal 2004;380:161–71.
- [39] Zhou Y, Li P, Goodwin AJ, Cook JA, Halushka PV, Chang E, Fan H. Exosomes from Endothelial Progenitor Cells Improve the Outcome of a Murine Model of Sepsis. Molecular therapy: the journal of the American Society of Gene Therapy 2018;26:1375–84.
- [40] Li S, Li H, Zhangdi H, Xu R, Zhang X, Liu J, Hu Y, Ning D, Jin S. Hair follicle-MSC-derived small extracellular vesicles as a novel remedy for acute pancreatitis. Journal of controlled release: official journal of the Controlled Release Society 2022;352:1104–15.
- [41] Han L, Zhao Z, Chen X, Yang K, Tan Z, Huang Z, Zhou L, Dai R. Human umbilical cord mesenchymal stem cells-derived exosomes for treating traumatic pancreatitis in rats. Stem cell research & therapy 2022;13:221.
- [42] Wang C, Zhang C, Liu L, X A, Chen B, Li Y, Du J. Macrophage-Derived mir-155-Containing Exosomes Suppress Fibroblast Proliferation and Promote Fibroblast Inflammation during Cardiac Injury. Molecular therapy: the journal of the American Society of Gene Therapy 2017;25:192–204.
- [43] Hu C, Meiners S, Lukas C, Stathopoulos GT, Chen J. Role of exosomal microRNAs in lung cancer biology and clinical applications. Cell proliferation 2020;53:e12828.
- [44] Chen J, Hu C, Pan P. Extracellular Vesicle MicroRNA Transfer in Lung Diseases. Frontiers in physiology 2017;8:1028.
- [45] Au Yeung CL, Co NN, Tsuruga T, Yeung TL, Kwan SY, Leung CS, Li Y, Lu ES, Kwan K, Wong KK, Schmandt R, Lu KH, Mok SC. Exosomal transfer of stroma-derived

- miR21 confers paclitaxel resistance in ovarian cancer cells through targeting APAF1. Nature communications 2016:7:11150.
- [46] Mittelbrunn M, Gutiérrez-Vázquez C, Villarroya-Beltri C, González S, Sánchez-Cabo F, González M, Bernad A, Sánchez-Madrid F. Unidirectional transfer of microRNA-loaded exosomes from T cells to antigen-presenting cells. Nature communications 2011:2:282.
- [47] Liu Y, Luo F, Wang B, Li H, Xu Y, Liu X, Shi L, Lu X, Xu W, Lu L, Qin Y, Xiang Q, Liu Q. STAT3-regulated exosomal miR-21 promotes angiogenesis and is involved in neoplastic processes of transformed human bronchial epithelial cells. Cancer letters 2016;370:125–35.
- [48] Hu H, Wang B, Jiang C, Li R, Zhao J. Endothelial progenitor cell-derived exosomes facilitate vascular endothelial cell repair through shuttling miR-21-5p to modulate Thrombospondin-1 expression. Clinical science (London, England: 1979) 2019;133:1629-44.
- [49] Hu Y, Rao SS, Wang ZX, Cao J, Tan YJ, Luo J, Li HM, Zhang WS, Chen CY, Xie H. Exosomes from human umbilical cord blood accelerate cutaneous wound healing through miR-21-3p-mediated promotion of angiogenesis and fibroblast function. Theranostics 2018;8:169–84.
- [50] Li W, Ma K, Zhang S, Zhang H, Liu J, Wang X, Li S. Pulmonary microRNA expression profiling in an immature piglet model of cardiopulmonary bypass-induced acute lung injury. Artificial organs 2015;39:327–35.
- [51] Zhou W, Su L, Duan X, Chen X, Hays A, Upadhyayula S, Shivde J, Wang H, Li Y, Huang D, Liang S. MicroRNA-21 down-regulates inflammation and inhibits periodontitis. Molecular immunology 2018;101:608–14.
- [52] Xue Z, Xi Q, Liu H, Guo X, Zhang J, Zhang Z, Li Y, Yang G, Zhou D, Yang H, Zhang L, Zhang Q, Gu C, Yang J, Da Y, Yao Z, Duo S, Zhang R. miR-21 promotes NLRP3 inflammasome activation to mediate pyroptosis and endotoxic shock. Cell death & disease 2019;10:461.
- [53] Pan T, Jia P, Chen N, Fang Y, Liang Y, Guo M, Ding X. Delayed Remote Ischemic Preconditioning Confers Renoprotection against Septic Acute Kidney Injury via Exosomal miR-21. Theranostics 2019;9:405–23.
- [54] Zhao Z, Hao J, Li X, Chen Y, Qi X. miR-21-5p regulates mycobacterial survival and inflammatory responses by targeting Bcl-2 and TLR4 in Mycobacterium tuberculosis-infected macrophages. FEBS letters 2019;593:1326–35.